Preprints (www.preprints.org) | NOT PEER-REVIEWED | Posted: 18 August 2018 doi:10.20944/preprints201808.0331.v1

Preparation, characterization, cytotoxicity and biological evaluation of ^{99m}Tc-Doxorubicin-Epigallocatechingallate functionalized gold nanoparticles as a new generation of theranostic radiopharmaceutical

Tamer M. Sakr*[1,2], Sherine A. G. Morsy[2], Nourhan A. Mahmoud[2], Hassan M. Rashed[3], H. A. Abd El-Rehim[4], Menka Khoobchandani[5], Kavita K. Katti[5], Kattesh V. Katti[5,6,7]*

[1]*Radioactive Isotopes and Generators Department, Hot Laboratories Centre, Atomic Energy Authority, P.O. Code 13759, Cairo, Egypt.*

[2] *Pharmaceutical Chemistry Department, Faculty of Pharmacy, October University of Modern Sciences and Arts (MSA), Giza, Egypt.*

[3]*Labeled Compounds Department, Hot Labs Center, Atomic Energy Authority, P.O. Box 13759, Cairo, Egypt.*

[4]Department of polymers, National Center for Radiation Research and Technology, Atomic Energy Authority, P.O. Box 13759, Cairo, Egypt.

[5]*Institute of Green Nanotechnology, Department of Radiology University of Missouri, Columbia, MO, 65212, USA.*

[6]*Missouri University Research Reactor, University of Missouri, Columbia, MO 65212, USA.*

[7]*Department Physics, University of Missouri, Columbia, MO, 65212, USA.*

**Corresponding authors E-mails: Tamer_sakr78@yahoo.com* (Tamer M. Sakr)

& KattiK@health.missouri.edu (Kattesh V. Katti)

© 2018 by the author(s). Distributed under a Creative Commons CC BY license.

Preprints (www.preprints.org) | NOT PEER-REVIEWED | Posted: 18 August 2018 doi:10.20944/preprints201808.0331.v1

Graphical abstract

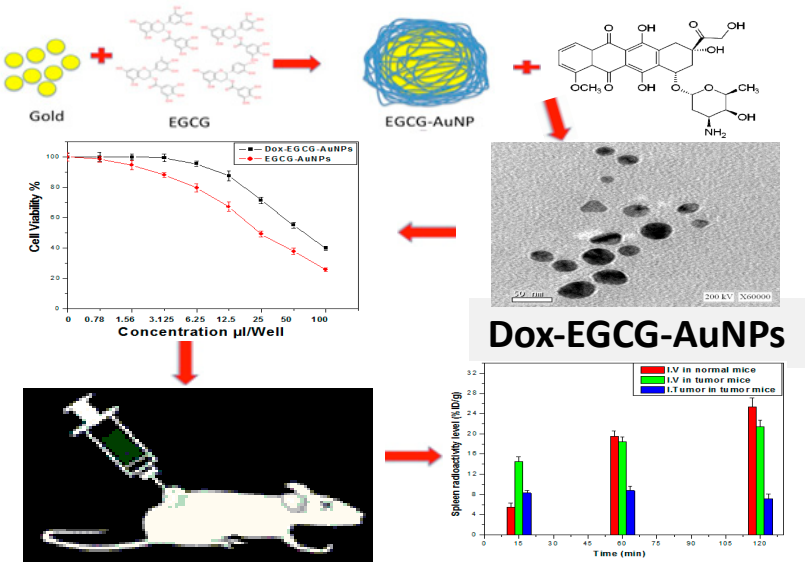

Abstract

Gold nanoparticles are currently used for the treatment of cancer through a myriad of modalities and delivery approaches. Conjugation of tumor imaging Single Photon Emitting Computed Tomographic (SPECT) radiopharmaceutical to gold nanoparticles will allow systemic targeting and imaging of cancer tissues simultaneously. In this study, gold nanoparticles (AuNPs) were prepared using Epigallocatechingallate (EGCG), loaded with doxorubicin (Dox), and characterized before and after doxorubicin conjugation. Cytotoxicity of EGCG-AuNPs and Dox-EGCG-AuNPs were evaluated against breast carcinoma (MCF-7) and hepatocellular carcinoma (HepG-2) cell lines demonstrating high cytotoxic effects of Dox-EGCG-AuNPs against both cell lines. Doxorubicin was radiolabeled with ^{99m}Tc and our new approach has optimized various labeling conditions resulting in a radiochemical yield of 93.5 ± 2.04%. Biodistribution of ^{99m}Tc-Dox-EGCG-AuNPs was studied in normal and tumor bearing mice following I.V. and intratumoral injections at different time intervals. Results showed high uptake of the intravenously injected ^{99m}Tc-Dox-EGCG-AuNPs in tumor tissue (22.45 %ID/g at 2h). In addition, localized intratumoral injection of ^{99m}Tc-Dox-EGCG-AuNPs showed extremely high levels of uptake in tumor (80.22 %ID/g at 15min) with high retention for extended periods post injection. Our results present prospects for the utility of ^{99m}Tc-Dox-EGCG-AuNPs as a multiplexed theranostic agent through SPECT imaging of tumor tissue and therapy through photothermal destruction of cancer tissue through the application of exogenous laser lights as well as through tyrosine phosphatases inhibitor (through EGCG), and topoisomerase II inhibitor (through doxorubicin) effects.

Keywords: Gold nanoparticles; EGCG; Doxorubicin; Radiolabeling; Theranostics

Preprints (www.preprints.org) | NOT PEER-REVIEWED | Posted: 18 August 2018 doi:10.20944/preprints201808.0331.v1

1. Introduction

Design and development of functionalized nanoparticles continues to be a burgeoning area of unparalleled growth because of continued applications within the health care, materials science, energy and environmental sectors[1-4]. Although a variety of nanoparticles encompass myriad of applications, certain types of nanoparticles with dual diagnostics and therapeutics, referred to as 'theranostics', have gained particular prominence in molecular imaging and therapy of cancers [1, 5-7]. Gold nanoparticles (AuNPs) for example are ideal candidates for therapeutic applications due to their inherent properties to emit heat upon irradiation with lasers/X-rays. The large surface area of gold nanoparticles allows incorporation of therapeutic agents thus making functionalized AuNPs as multiplexed therapeutic agents [8-11]. Katti et.al. have shown the application of AuNPs as X-ray contrast agents thus opening up new opportunities in the utility of functionalized AuNPs as theranostic agents [5, 12].Katti et al have also demonstrated the development of radioactive gold nanoparticles (Au-198) with beta and gamma emission properties for theranostic applications in molecular imaging and therapy of cancers [1]. Recent studies have also shown that gold nanoparticles functionalized with tumor receptor specific peptides or receptor-avid small biomolecules, when injected directly into tumors, are retained within the tumor in significant amounts. Such intratumoral delivery approaches would be ideally suited for treating solid tumors (prostate, hepatic, glioblastoma, etc) because of the potential to reduce damage to healthy cells [13, 14]. Nanotechnology appears to offer new avenues for the development of intratumorally injectable paradigm thus overcoming existing challenges of drug delivery, which suffer from difficulties of optimal uptake of drugs at the tumor site due to various physiological barriers.

Recent studies have shown that gold nanoparticles (AuNPs) are considered a clear choice in intratumroal drug delivery due to their ability to be functionalized with a variety of tumor-avid biomolecules, ideal hydrodynamic size for penetration across tumor cell membranes, and efficient matrix/receptors mediated active and passive internalization [9, 15, 16]. Recent studies on the efficacy of functionalized gold nanoparticles in treating various cancers provide illustrious examples about the realistic scope of gold-based nanomedicine in tumor therapy [17-21]. Certain phytochemicals such as Epigallocatechingallate (EGCG) from tea are electron rich. Katti et. al. have demonstrated the extraordinary electron injection capability of EGCG to transform gold into gold nanoparticles, through innovative green nanotechnology, with concomitant encapsulation of tumor-avid phytochemical on the surface [22-26].

Highly reactive and the vast surface area of gold nanoparticles allows effective conjugations with the FDA approved chemotherapeutic agents including Doxorubicin (DOX) [27-32]. Doxorubicin is a chemotherapeutic agent being currently used for treating multiple types of cancers including breast cancer, bladder cancer, ovarian cancer, lymphoma, and acute lymphocytic leukemia. Common side effects of doxorubicin include cardiotoxicity, hair loss, bone marrow suppression, vomiting, rash, and inflammation of the mouth[33, 34]. An important consideration is that conjugating doxorubicin with gold nanoparticles might reduce its side effects due to passive targeting of cancer tissue aided through enhanced permeability and retention effects (EPR) [35, 36]. In addition, attaching doxorubicin to gold nanoparticles provides a dual mode of treatment of cancer involving both the chemotherapeutic effects of doxorubicin as well as thermally-mediated cancer cell killing destructive effects of gold nanoparticles [37, 38]. Gold nanoparticulates functionalized with doxorubicin would also present attractive prospects for labeling with Single Photon Emitting Computed Tomographic (SPECT) radioisotopes such as ^{99m}Tc. ^{99m}Tc radiopharmaceuticals provide excellent SPECT images of tumors/lesions [39-41]. Therefore, multiplexing of doxorubicin-loaded gold nanoparticles and subsequent labeling of such therapeutic conjugates with ^{99m}Tc opens up new avenues in the design and

Preprints (www.preprints.org) | NOT PEER-REVIEWED | Posted: 18 August 2018 doi:10.20944/preprints201808.0331.v1

development of theranostic agents with applications in oncology [42-46]. We, herein, report the development of gold nanoparticles functionalized doxorubicin and its subsequent labeling with ^{99m}Tc to produce a new generation of a theranostic nano-radiopharmaceutical (^{99m}Tc-Dox-EGCG-AuNPs). We also report full details of biodistribution of ^{99m}Tc-Dox-EGCG-AuNPs in normal and tumor bearing mice following I.V and intratumoral injection at different time intervals. Our results provide new directions in oncology for the utility of ^{99m}Tc-Dox-EGCG-AuNPs as a theranostic agent through SPECT imaging of tumor tissue and therapy through the conjugated Doxorubicin as well as through the photothermal destruction of cancer tissue through the application of exogenous laser lights.

2. Results and discussion:

2.1. Preparation of gold nanoparticles (EGCG-AuNPs)

EGCG-AuNPs were prepared following a protocol we have developed in our laboratory [20, 58]. This preparation was optimized by mixing 300 µL of EGCG solution with 60 µl $NaAuCl_4.2H_2O$ solution until the formation of ruby red color indicating the formation of gold particles in the optimum nano size. Finally the prepared EGCG-AuNPs solution was diluted to 2 ml using physiological solution.

2.2. Preparation of EGCG-AuNPs loaded with doxorubicin

DOX is adsorbed onto EGCG-AuNPs mainly through electrostatic interactions between the positively charged amine group of DOX and the negatively charged polyphenolics groups of EGCG, used in the synthesis as a reducing and stabilizing agents [59, 60]. The hydrophobic forces drive the doxorubicin molecule to the surface of the EGCG-AuNPs which has a strong corona of negatively charged polyphenols of EGCG to produce a robust and stable electrostatic interaction between DOX-EGCG-AuNPs (**Figure 1**) [61]. Several key features must be considered for nanoscale-drug conjugates to be successful in animal-based models. First, the size of the nanoparticle complex must remain in nano range of 10-100 nm for effective penetration of ^{99m}Tc-DOX-EGCG-AuNPs mediated by EPR effects. In addition, the nanoparticle must be stable in the high ionic strength environments present *in-vivo*. Secondly, controlled release of the drug at the target site must be guaranteed. The effective adsorption and electrostatic interaction of DOX with EGCG corona onto gold nanoparticles appear to provide ideal size, stability for the controlled release of DOX at tumor sites. Upon adsorption of high concentration of DOX onto EGCG corona conjugated to EGCG-AuNPs, the overall *in-vitro* and the *in-vivo* stability is enhanced with limited or no aggregation.

Overall, we have succeeded in loading EGCG-AuNPs with 0.4 ml of doxorubicin solution, which is equivalent to 0.4 mg doxorubicin, without compromising its stability.

Preprints (www.preprints.org) | NOT PEER-REVIEWED | Posted: 18 August 2018 doi:10.20944/preprints201808.0331.v1

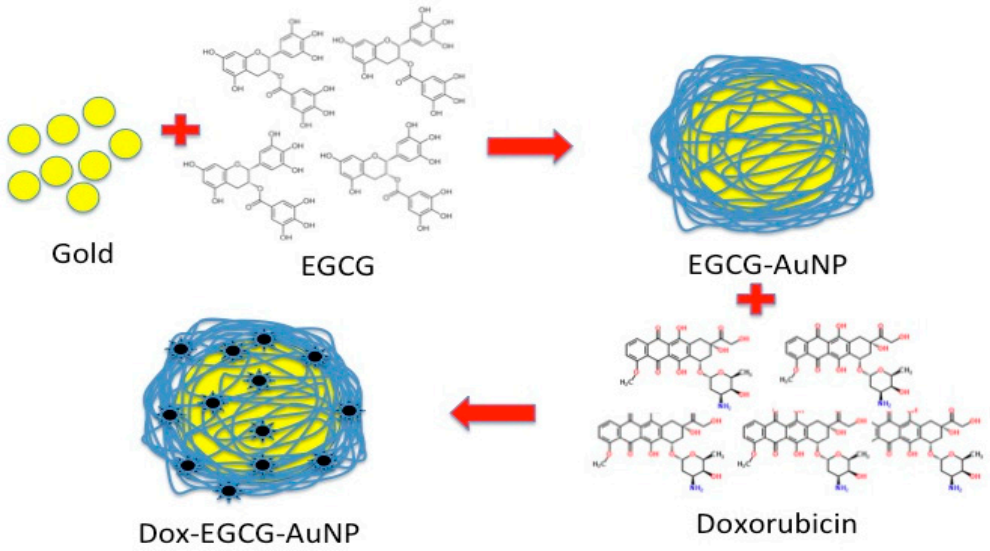

Figure 1: Illustrative diagram showing multiplexed conjugations of EGCG on AuNPs and subsequent loading with Doxorubicin to produce the theranostic agent: Dox-EGCG-AuNP

2.3. Characterization of EGCG-AuNPs and Dox-EGCG-AuNPs

Figure 2 shows the DLS, TEM and IR charts of EGCG-AuNPs and Dox-EGCG-AuNPs. The EGCG-AuNPs nanoparticles, as measured through dynamic light scattering (DLS) experiments, showed a mean diameter of 21.4±1 nm which is within the optimum nano-size allowing ready diffusion across the cancer leaky cancer cell vessels with minimal hindrance [62, 63]. Furthermore, the DLS analysis of the Dox-EGCG-AuNPs showed mean diameter of 58.9±2 nm indicating a significant increase in particle size suggesting Dox loading onto the EGCG-AuNPs. It is important to recognize that the overall size of Dox-EGCG-AuNPsis still within the optimum range, allowing efficient penetration, through receptor-mediated endocytosis as well as through EPR effects, to provide optimum doses of theranostic drugs to tumor cells.

TEM (transmission electron microscopy) analysis is a useful tool for examining the morphological characteristics of nanoparticles. **Figure 2** showed non-aggregated EGCG-AuNPs and Dox-EGCG-AuNPs with a predominant spherical shape and narrow size distribution, besides; electronic microscopy clearly showed that the diameter of the particles observed through TEM measurements were in harmony with those measured through DLS analysis (Figure 2).

The IR chart revealed that similarity between EGCG-AuNPs and Dox-EGCG-AuNPs preparations.

Preprints (www.preprints.org) | NOT PEER-REVIEWED | Posted: 18 August 2018 doi:10.20944/preprints201808.0331.v1

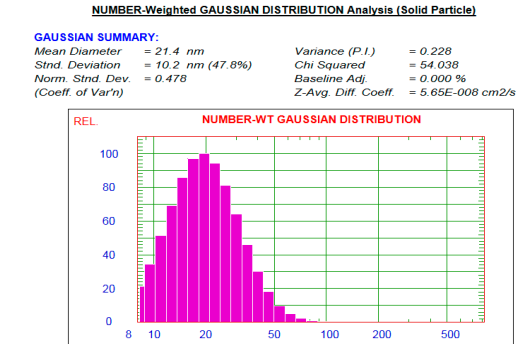

(a) DLS analysis of EGCG-AuNPs

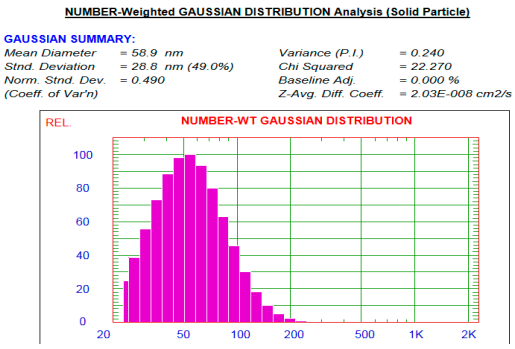

(b) DLS analysis of Dox-EGCG-AuNPs

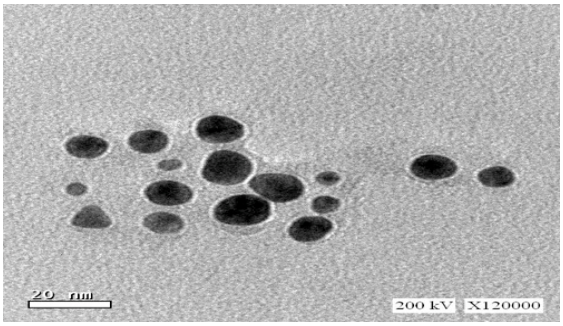

(c) TEM image of EGCG-AuNPs

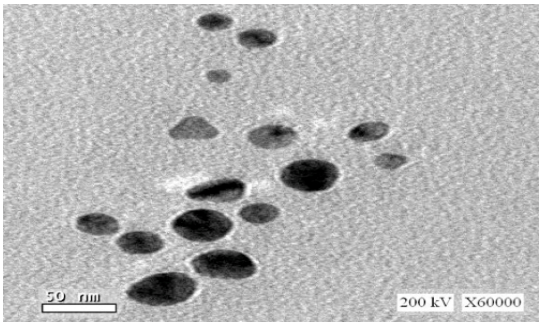

(d) TEM image of Dox-EGCG-AuNPs

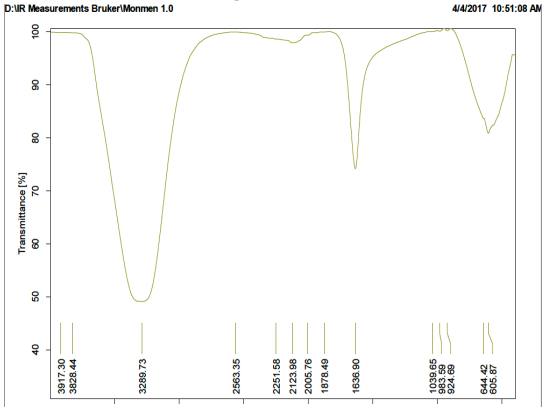

(e) IR chart of EGCG-AuNPs

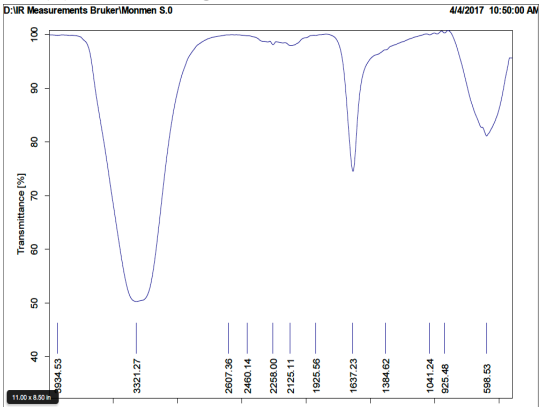

(f) IR chart of Dox-EGCG-AuNPs

Figure 2:DLS, TEM and IR charts of EGCG-AuNPs and Dox-EGCG-AuNPs

2.4. In-vitro cytotoxicity of EGCG-AuNPs and Dox-EGCG-AuNPs

Results of in vitro cytotoxicity revealed enhanced inhibitory activity of Dox-EGCG-AuNPs (IC_{50} =40.78±1.40 µl/Well) against breast carcinoma MCF-7 cell line. These cytotoxicity effects are significantly more pronounced than those observed for EGCG-AuNPs (IC_{50} =79.8±1.59 µl/Well) (**Figure 3a**). In addition, similar anti-tumor enhancements for Dox-EGCG-AuNPs were obtained in the cytotoxicity studies against hepatocellular carcinoma HepG-2 cell line with IC_{50}=66.7±5.78 µl/Well for EGCG-AuNPs and IC_{50}=24.4±2.35 µl/Well for Dox-EGCG-AuNPs(**Figure 3b**).

Preprints (www.preprints.org) | NOT PEER-REVIEWED | Posted: 18 August 2018 doi:10.20944/preprints201808.0331.v1

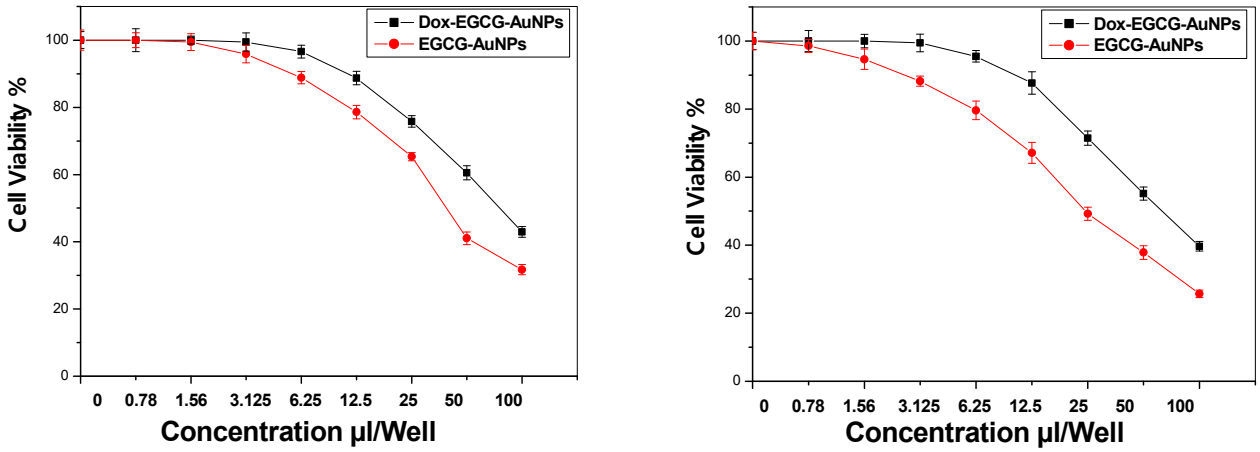

(a) **(b)**

Figure 3: Evaluation of cytotoxicity of EGCG-AuNPs and Dox-EGCG-AuNPs against (a) MCF-7 cell line; (b) HepG-2 cell line

2.5. Radiolabeling of doxorubicin using ^{99m}Tc

Optimum radiochemical yield of 93.5 ± 2.04% was obtained using 1 mg doxorubicin and 100 µg stannous chloride at 15 min reaction time, room temperature and pH 7 (**Figure 4**). ^{99m}Tc-doxorubicin showed good *in-vitro* stability up to 6 h.

Preprints (www.preprints.org) | NOT PEER-REVIEWED | Posted: 18 August 2018 doi:10.20944/preprints201808.0331.v1

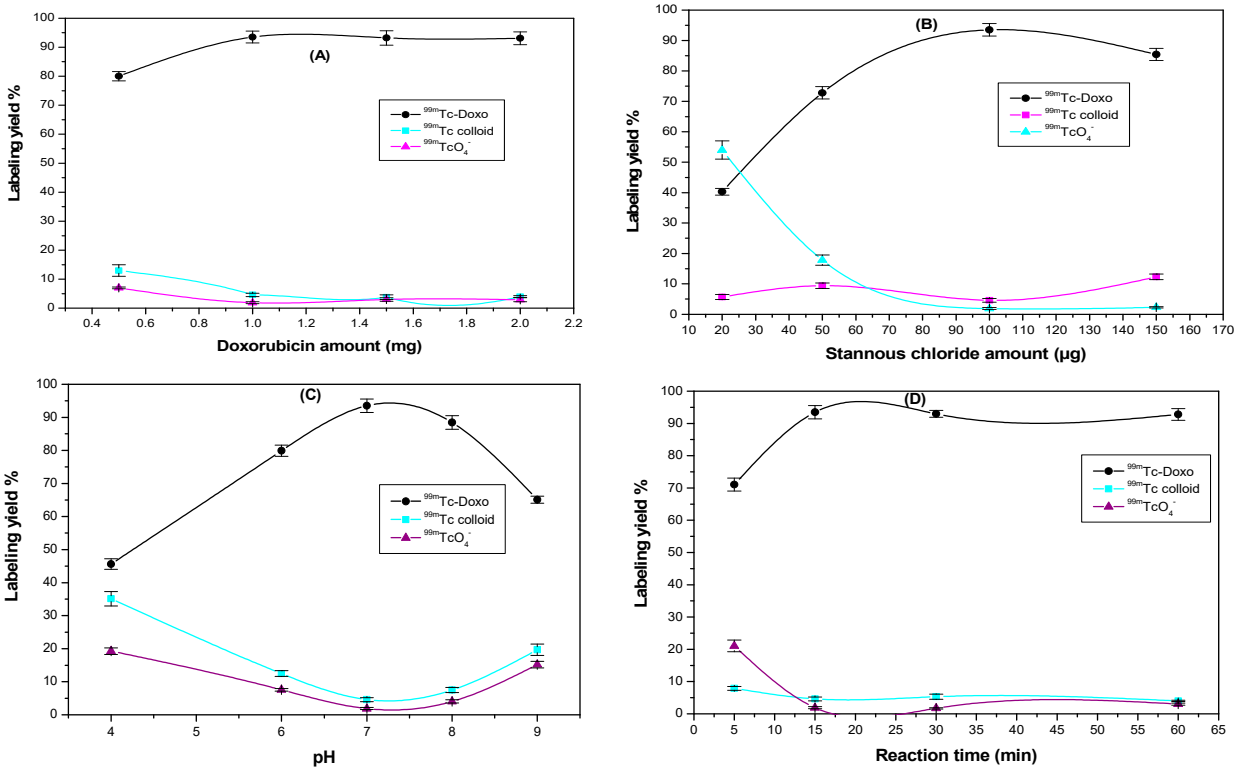

Figure 4: Variation of RCY of ^{99m}Tc-Dox as a function of doxorubicin amount, stannous chloride amount, pH and time (A-D)

2.6. In-vitro stability of ^{99m}Tc-Dox-EGCG-AuNPs

In vitro stability evaluations of ^{99m}Tc-Dox-EGCG-AuNPs were carried out in saline and rat serum. ^{99m}Tc-Dox-EGCG-AuNPs showed excellent *in-vitro* stability in saline and in rat serum for 3 days. Radiochemical yields of ^{99m}Tc-Dox-EGCG-AuNPs remained unchanged over three days period. The optimum in vitro stability of ^{99m}Tc-Dox-EGCG-AuNPs provides compelling rationale for a detailed in vivo investigations of this theranostic agent in tumor bearing mice.

2.7. Biodistribution study of ^{99m}Tc-Dox-EGCG-AuNPs

Results of biodistribution studies revealed substantial accumulation of ^{99m}Tc-Dox-EGCG-AuNPs in tumor tissue (22.45 %ID/g at 2h) **(Figure 5)**. This targeting efficacy selectively to tumor sites is attributed to active targeting enhanced by doxorubicin as well as gold nanoparticles-mediated passive targeting due to enhanced permeability and retention (EPR) effects [64-67]. On the other hand, localized intratumoral injections of ^{99m}Tc-Dox-EGCG-AuNPs showed extremely high level of radioactivity uptake in tumor tissue (80.22 %ID/g at 15min) and remained at that level for 2 hr post injection. These promising tumor targeting and retention data indicate the usefulness of ^{99m}Tc-Dox-EGCG-AuNPs as a theranostic agent (**Figure 5 and 6**). The ^{99m}Tc SPECT probe in ^{99m}Tc-Dox-EGCG-AuNPs molecular imaging of lesions particularly for early diagnosis of tumors as well as for follow up in monitoring therapeutic response in cancer patients [68-70]. Besides, our overall approach has multiplexed dimension due to the presence of gold nanoparticles which allow their use for photothermal destruction of cancer tissue when exogenous laser lights are applied [71, 72].

Preprints (www.preprints.org) | NOT PEER-REVIEWED | Posted: 18 August 2018 doi:10.20944/preprints201808.0331.v1

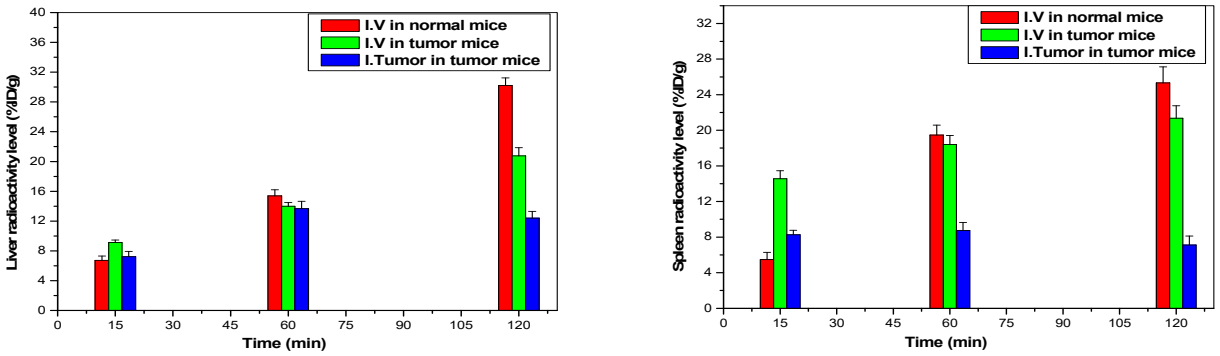

(a) **(b)**

Figure 5: Liver uptake (a); Spleen uptake (b) of ^{99m}Tc-Dox-EGCG-AuNPs in normal and tumor bearing mice following I.V and intra-tumor injection at different time intervals

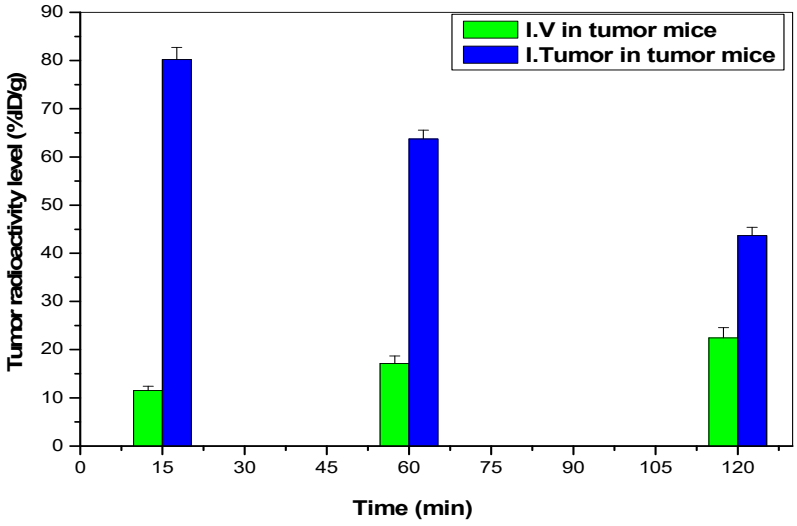

Figure 6: Tumor uptake of ^{99m}Tc-Dox-EGCG-AuNPs in tumor bearing mice following I.V. and intra-tumor injection at different time intervals

2.8 Synergistic multiplexing therapeutic and imaging of ^{99m}Tc-Dox-EGCG-AuNPs:

The ability of doxorubicin to exert its antitumor effects *via* inhibition of topoisomerase II continues to attract significant clinical interest for its applications as the most important anticancer drug in the clinic [28]. Unfortunately, its potent antitumor activity is also accompanied by severe systemic short and long-term tissue toxicities including cardiotoxicity. In addition, shorter intracellular retention time, as noted in a number of clinical investigations of doxorubicin, has been the main vexing medical problem in exploiting the full clinical potential of this class of anthracycline compounds in tumor therapy. Limited tumor retention is often overcome by repeated doses causing dose-limiting side effects in the form of cardiotoxicity, leading to heart failure in the most severe cases.

Extensive preclinical studies have demonstrated that chronic administration of doxorubicin would result in a severe DRG (dorsal root ganglia) neuronopathy [33, 34]. Therefore, current and future clinical applications

Preprints (www.preprints.org) | NOT PEER-REVIEWED | Posted: 18 August 2018 doi:10.20944/preprints201808.0331.v1

of doxorubicin, as a first line cancer therapy drug, requires development of delivery technologies that would not only result in selective delivery at tumor sites but also enhance retention of therapeutic doses with minimal/no systemic side effects. Biodistribution and tumor retention results of ^{99m}Tc-Dox-EGCG-AuNPs provide conclusive evidence that conjugation of doxorubicin with tumor targeting EGCG provides selective delivery at the same time enhance the retention of optimal therapeutic doses of this drug (**Figures 5 and 6**). The gold nanoparticles in ^{99m}Tc-Dox-EGCG-AuNPs, to which doxorubicin is tagged with, also provide synergistic advantages of both tumor targeting and retention of doxorubicin because of the well-known affinity of gold nanoparticulate surface to the leaky vasculature found on tumor cells. The selective affinity of EGCG to tumor cell receptors also provides selective affinity of the ^{99m}Tc SPECT probe of ^{99m}Tc-Dox-EGCG-AuNPs, thus providing for the first time, a functional doxorubicin-gold nanoparticulate-based SPECT theranostics agent for dual imaging and therapy applications in the treatment of a myriad of cancers. The well-established chemotherapeutic effects of EGCG are also put to advantage in the theranostics action of ^{99m}Tc-Dox-EGCG-AuNPs

It is well known that receptor tyrosine kinases (RTKs) are the tumor proliferation machinery as they are directly involved in cell proliferation, survival and angiogenesis. The fact that EGCG regulates activities of cell surface growth factor receptors, especially receptor tyrosine kinases (RTK), including epidermal growth factor receptor (EGFR), vascular endothelial growth factor receptor (VEGFR), insulin-like growth factor receptor (IGFR), and the insulin receptor (InsR) [73-76] individually and collectively present unprecedented opportunities in the application of ^{99m}Tc-Dox-EGCG-AuNPs agent as a multiplex tyrosine phosphatases inhibitor (through EGCG), and topoisomerase II inhibitor (through doxorubicin) [28].

3. Materials and Methods:

3.1. Materials

Epigallocatechingallate (EGCG), Sodium tetrachloroaurate dehydrate and Doxorubicin are purchased from Sigma-Aldrich Company, USA. All other chemicals and solutions were of analytical grade and purchased from Merck Co. Fetal Bovine serum, DMEM, RPMI-1640, HEPES buffer solution, L-glutamine, gentamycin and 0.25% Trypsin-EDTA were purchased from Lonza, Whatman No.1 paper chromatography, Whatman International Ltd, Maidstone, Kent, UK.

3.1.1. Radioactive material

^{99}Mo/^{99m}Tc generator is purchased from Egyptian Atomic Energy Authority as a source of $^{99m}TcO_4^-$.

3.1.2. Equipment

Transmission electron microscopy (TEM; JEOL JEM-100CX, Japan). RT-IR, JASCO FT/IR-6300 spectrometer in the range of 400–4000 cm^{-1}. Dynamic Light Scattering (DLS) technique using a PSSNICOMP Zeta Potential/Particle Sizer 380ZLS (PSS-NICOMP, Santa Barbara, CA, USA). A NaI (Tl) γ-ray scintillation counter (Scaler Ratemeter SR7 model, UK).

3.1.3. Cell lines

Mammalian cell lines: MCF-7 cell line (human breast cancer) and **HepG-2**cell line ((human hepatocellular carcinoma) were purchased from the American Type Culture Collection (ATCC, Rockville, MD).

Preprints (www.preprints.org) | NOT PEER-REVIEWED | Posted: 18 August 2018 doi:10.20944/preprints201808.0331.v1

3.1.4. Animals

Male Swiss albino mice (20-40 gm) were used for the biodistribution studies that confirmed to the ethical guidelines for animal care set by the EAEA. Ehrlich Ascites Carcinoma tumor line solution ($12.5x10^6$ cells/mL) was injected intramuscularly (0.2 mL) in the right thigh to produce a solid tumor. It took about 10-15 days for the solid tumor to be apparent in the right thigh muscle [47].

3.2. Methods

3.2.1. Preparation of gold nanoparticles (EGCG-AuNPs)

Two separate solutions were prepared by dissolving 10mg of EGCG in10 mL of absolute ethanol (Solution A) and dissolving 10 mg of sodium tetrachloroaurate dehydrate in 10mL of double-distilled water (solution B). We choose EGCG due to its dual action as a reducing and also as a stabilizing agent in addition to its inherent property as an anticancer agent [23, 48-50]. Gold nanoparticles were prepared by drop wise addition of different volumes of solution B to different volumes of solution A in a 10 mL vial placed on a magnetic hot plate with stirring for about 15 min until a ruby red color appeared. The EGCG-AuNPs preparation was optimized after studying the effect of EGCG amount, gold amount, reaction time and reaction temperature factors. Then the prepared EGCG-AuNPs solution was diluted with physiological solution.

3.2.2. Preparation of EGCG-AuNPs loaded with doxorubicin (Dox-EGCG-AuNPs)

After the formation of EGCG-AuNPs, using different amounts of doxorubicin solution in H_2O (1 mg/mL) was added with magnetic stirring to evaluate the maximum amount of doxorubicin that can be loaded on EGCG-AuNPs.

3.2.3. Characterization of EGCG-AuNPs and Dox-EGCG-AuNPs

Transmission electron microscope (TEM), NICOMP Dynamic light scattering (DLS), and infrared spectroscopy (IR) were used to characterize the formed EGCG-AuNPs and Dox-EGCG-AuNPs.

3.2.4. In-vitro cytotoxicity study of gold nanoparticles and doxorubicin-gold nanoparticles cell line propagation

Medium of RPMI-1640 supplemented with 10% inactivated fetal calf serum and 50µg/mL gentamycin was used for cells growth. In a humidified atmosphere, cells were maintained at 37ºC and 5% CO_2 and sub-culturing was done two to three times a week.

3.2.5. Cytotoxicity evaluation using viability assay

For antitumor assays, the tumor cell lines were suspended at concentration $5x10^4$ cells/well in medium of Corning® 96-well tissue culture plates and incubated for 24 hr. The compounds to be examined were added into 96-well plates (three replicates) to achieve eight dilutions for each compound. The numbers of viable cells after 24 h incubation were determined by the MTT test. Media was removed from the 96 well plates and replaced with 100 µL of fresh culture RPMI 1640 medium without phenol red then 10 µL of 12 mM MTT stock solution (5 mg of MTT in 1 mL of PBS) added to each well including the untreated controls. The 96 well plates were then incubated at 37°C and 5% CO_2 for 4 hours. Then, 85 µl aliquot of the media was removed from the wells, and 50 µL of DMSO was added to each well and mixed thoroughly with the pipette and incubated at 37°C for 10 min.

Preprints (www.preprints.org) | NOT PEER-REVIEWED | Posted: 18 August 2018 doi:10.20944/preprints201808.0331.v1

Then, the optical density was measured at 590 nm with the microplate reader (SunRise, TECAN, Inc, USA) to determine the number of viable cells and the percentage of viability was calculated as [1-(ODt/ODc)]x100% where ODt is the mean optical density of wells treated with the sample and ODc is the mean optical density of untreated cells. The surviving cells percentage was plotted versus drug concentration to get the survival curve for each compound. The 50% inhibitory concentration (IC50) was estimated from graphic plots of the dose response curve for each concentration using Graphpad Prism software (San Diego, CA. USA) [51, 52].

3.2.6. Radiolabeling of doxorubicin using ^{99m}Tc

Radiolabeling of doxorubicin with ^{99m}Tc was done by direct technique under reductive conditions using $SnCl_2.2H_2O$ [53]. Labeling reaction was done by adding 1 mL of doxorubicin solution in DMSO (0.5-2 mg doxorubicin) in an evacuated 10 mL penicillin vial. Then, 7.2 MBq of $^{99m}TcO_4^-$ (100 µL of generator eluate) was added to each reaction. Initiation of the reaction was achieved by adding 0.5 ml stannous chloride solution (20-150 µg $SnCl_2.2H_2O$). Effect of reaction pH on radiochemical yield (RCY) was studied in range of 4-9 using different amounts of 0.1N sodium hydroxide or 0.1N hydrochloric acid solutions. Reaction time effect on radiolabeling yield was also studied (5-60 min). Ascending paper chromatography was used for analysis of RCY using acetone as a mobile phase to determine free $^{99m}TcO_4^-$% and water:ethanol:ammonia mixture (5:2:1 v:v:v) to determine colloidal impurities percentage [54, 55].

3.2.7. Preparation of EGCG-AuNPs loaded with ^{99m}Tc-doxorubicin (^{99m}Tc-Dox-EGCG-AuNPs)

Various stoichiometric amounts of ^{99m}Tc-doxorubicin and EGCG-AuNPs were mixed in order to arrive at an optimized preparation of ^{99m}Tc-Dox-EGCG-AuNPs. The highest loading of Doxorubicin onto ^{99m}Tc-Dox-EGCG-AuNPs was achieved by mixing 0.4 mL of the radiolabeled^{99m}Tc-doxorubicin solution with 1 mL of EGCG-AuNPs solution with magnetic stirring for 20 min.

3.2.8. In-vitro stability of ^{99m}Tc-Dox-EGCG-AuNPs

Before going through the *in-vivo* evaluations, the *in-vitro* stability of the ^{99m}Tc-Dox-EGCG-AuNPs was conducted in saline and rat serum to confirm its suitability for *in-vivo* injections.^{99m}Tc-Dox-EGCG-AuNPs was examined for *in-vitro* stability in saline and rat serum by mixing 0.1 mL of each preparation with 0.9 mL of saline or rat serum for 1 week.

3.2.9. Biodistribution study of ^{99m}Tc-Dox-EGCG-AuNPs

Mice were classified into three groups (9 mice/group) A, B and C. Line of Ehrlich Ascites Carcinoma was used to induce solid tumor in mice of groups B and C while group A is considered as normal group. The parent tumor line was withdrawn from 7 days old donor female Swiss Albino mice and diluted with sterile physiological saline solution to give 12.5 X 10^6 cells/ml. Exactly 0.2 mL solution was then injected intramuscularly in the right thigh muscle to produce a solid tumor. The animals were maintained till the tumor development was apparent (10-15 day) [47].

On the experiment day, nearly 6.2 MBq of^{99m}Tc-Dox-EGCG-AuNPs (150 µl) were injected intravenously in group A mice, intravenously in group B mice and finally intra tumor injection in group C mice at 15, 60 and 120 minutes (three mice/time interval). Each mouse was weighed, anaesthetized by chloroform, euthanized and then dissected. Different body organs were separated, weighed and rinsed with saline. Uptake of radioactivity in each organ was measured using a gamma counter and expressed as percent injected dose per gram (% ID/gram ±

Preprints (www.preprints.org) | NOT PEER-REVIEWED | Posted: 18 August 2018 doi:10.20944/preprints201808.0331.v1

S.D.)[56, 57]. One-way ANOVA test (P<0.05) was used to evaluate data and all the results were given as mean ± SEM.

4. Conclusions

Doxorubicin-EGCG functionalized gold nanoparticles were successfully prepared using EGCG as a reducing and stabilizing agent and characterized through DLS, TEM and IR spectroscopy. Doxorubicin-EGCG functionalized gold nanoparticles showed excellent cytotoxic effects against MCF-7 and HepG-2 cell lines. Doxorubicin-EGCG functionalized gold conjugate was successfully radiolabeled using ^{99m}Tc achieving high radiochemical yields of 93.5 ± 2.04%. Biological behavior of ^{99m}Tc-Dox-EGCG-AuNPs in tumor bearing mice showed high targeting ability towards cancer tissue after I.V and intratumoral administrations with substantial accumulation and retention of diagnostic and therapeutic doses in tumor site. Our results demonstrate the applications of ^{99m}Tc-Dox-EGCG-AuNPs in oncology as a new generation of theranostic agent allowing synchronous SPECT imaging, photothermal therapy (through gold nanoparticles), as well as tyrosine phosphatases inhibitor (through EGCG), and topoisomerase II inhibitor (through doxorubicin) therapeutics.

Conflict of interest:

All authors declared no conflict of interest.

Ethical approval:

Authors report that all applicable international and institutional guidelines for the care and use of animals were followed.

Acknowledgment

Tamer M. Sakr, Hassan A. Abd El-Rehim and Kattesh V. Katti express their grateful appreciation and thanks for International Atomic Energy Authority (IAEA) for international collaboration and funding this work under CRP No. F22064.

Kattesh V.Katti acknowledges funds from the Institute of Green Nanotechnology, University of Missouri, Columbia, USA.

References

1. Katti, K.V., *Renaissance of nuclear medicine through green nanotechnology: functionalized radioactive gold nanoparticles in cancer therapy-my journy from chemistry to saving human lives.* Journal of Radioanalytical and Nuclear Chemistry, 2016. **309**: p. 5-14.

2. Reiss, G. and A. Hütten, *Magnetic nanoparticles: applications beyond data storage.* Nature materials, 2005. **4**(10): p. 725.

Preprints (www.preprints.org) | NOT PEER-REVIEWED | Posted: 18 August 2018 doi:10.20944/preprints201808.0331.v1

3. Das, M., N. Saxena, and P.D. Dwivedi, *Emerging trends of nanoparticles application in food technology: Safety paradigms.* Nanotoxicology, 2009. **3**(1): p. 10-18.

4. Stark, W.J., et al., *Industrial applications of nanoparticles.* Chemical Society Reviews, 2015. **44**(16): p. 5793-5805.

5. Chanda, N., et al., *Gold nanoparticle based X-ray contrast agent for tumor imaging in mice and dog: a potential nanoplatform for computer tomography theranostics.* Journal of biomedical nanotechnology, 2014. **10**(3): p. 383-392.

6. Tong, R. and J. Cheng, *Anticancer polymeric nanomedicines.* Journal of Macromolecular Science, Part C: Polymer Reviews, 2007. **47**(3): p. 345-381.

7. Wagner, E., *Programmed drug delivery: nanosystems for tumor targeting.* Expert opinion on biological therapy, 2007. **7**(5): p. 587-593.

8. Cheng, C.J., et al., *A holistic approach to targeting disease with polymeric nanoparticles.* Nature reviews Drug discovery, 2015. **14**(4): p. 239.

9. Daraee, H., et al., *Application of gold nanoparticles in biomedical and drug delivery.* Artificial cells, nanomedicine, and biotechnology, 2016. **44**(1): p. 410-422.

10. Mou, X., et al., *Applications of magnetic nanoparticles in targeted drug delivery system.* Journal of nanoscience and nanotechnology, 2015. **15**(1): p. 54-62.

11. Yameen, B., et al., *Insight into nanoparticle cellular uptake and intracellular targeting.* Journal of Controlled Release, 2014. **190**: p. 485-499.

12. Kattumuri, V., et al., *Stabilized gold nanoparticle and contrast agent*. 2017, Google Patents.

13. Amjad, M.S., et al., *Nano particles: An emerging tool in biomedicine.* Asian Pacific Journal of Tropical Disease, 2015. **5**(10): p. 767-771.

14. Anselmo, A.C. and S. Mitragotri, *Cell-mediated delivery of nanoparticles: taking advantage of circulatory cells to target nanoparticles.* Journal of Controlled Release, 2014. **190**: p. 531-541.

15. Tiwari, P.M., et al., *Functionalized gold nanoparticles and their biomedical applications.* Nanomaterials, 2011. **1**(1): p. 31-63.

16. Zhang, X., *Gold nanoparticles: recent advances in the biomedical applications.* Cell biochemistry and biophysics, 2015. **72**(3): p. 771-775.

17. Boote, E., et al., *Gold nanoparticle contrast in a phantom and juvenile swine: models for molecular imaging of human organs using x-ray computed tomography.* Academic radiology, 2010. **17**(4): p. 410-417.

Preprints (www.preprints.org) | NOT PEER-REVIEWED | Posted: 18 August 2018 doi:10.20944/preprints201808.0331.v1

18. Jazayeri, M.H., et al., *Various methods of gold nanoparticles (GNPs) conjugation to antibodies.* Sensing and bio-sensing research, 2016. **9**: p. 17-22.

19. Salouti, M. and F. Saghatchi, *BBN conjugated GNPs: a new targeting contrast agent for imaging of breast cancer in radiology.* IET nanobiotechnology, 2017. **11**(5): p. 604-611.

20. Shukla, R., et al., *Laminin receptor specific therapeutic gold nanoparticles (198AuNP-EGCg) show efficacy in treating prostate cancer.* Proceedings of the National Academy of Sciences, 2012. **109**(31): p. 12426-12431.

21. Thakor, A., et al., *Gold nanoparticles: a revival in precious metal administration to patients.* Nano letters, 2011. **11**(10): p. 4029-4036.

22. Katti, K.V., et al., *Egcg stabilized gold nanoparticles, therapies and sensing*. 2016, Google Patents.

23. Khoobchandani, M., et al., *Laminin receptor-avid nanotherapeutic EGCg-AuNPs as a potential alternative therapeutic approach to prevent restenosis.* International journal of molecular sciences, 2016. **17**(3): p. 316.

24. Khoobchandani, M., et al., *Green Nanotechnology from Brassicaceae: Development of Broccoli Phytochemicals–Encapsulated Gold Nanoparticles and Their Applications in Nanomedicine.* International Journal of Green Nanotechnology, 2013. **1**: p. 1943089213509474.

25. Makarov, V., et al., *"Green" nanotechnologies: synthesis of metal nanoparticles using plants.* Acta Naturae (англоязычная версия), 2014. **6**(1 (20)).

26. Shah, M., et al., *Green synthesis of metallic nanoparticles via biological entities.* Materials, 2015. **8**(11): p. 7278-7308.

27. Jo, A., et al., *Inhibition of carbonyl reductase 1 safely improves the efficacy of doxorubicin in breast cancer treatment.* Antioxidants & redox signaling, 2017. **26**(2): p. 70-83.

28. Mikhail, A.S., et al., *Lyso-thermosensitive liposomal doxorubicin for treatment of bladder cancer.* International Journal of Hyperthermia, 2017. **33**(7): p. 733-740.

29. Nikoobakht, B., *Methods and apparatuses for surface functionalization and coating of nanocrystals*. 2015, Google Patents.

30. Siddiqi, K.S. and A. Husen, *Recent advances in plant-mediated engineered gold nanoparticles and their application in biological system.* Journal of Trace Elements in Medicine and Biology, 2017. **40**: p. 10-23.

31. Wang, L., et al., *Multifunctional telodendrimer nanocarriers restore synergy of bortezomib and doxorubicin in ovarian cancer treatment.* Cancer research, 2017. **77**(12): p. 3293-3305.

32. Xu, P., et al., *Doxorubicin-Loaded Platelets Conjugated with Anti-CD22 Mabs: A Novel Targeted Delivery System for B-Cell Lymphoma Treatment with Cardiac Avoidance*. 2017, Am Soc Hematology.

Preprints (www.preprints.org) | NOT PEER-REVIEWED | Posted: 18 August 2018 doi:10.20944/preprints201808.0331.v1

33. Brand, W., et al., *Nanomedicinal products: A survey on specific toxicity and side effects.* International journal of nanomedicine, 2017. **12**: p. 6107.

34. Zhu, C., et al., *Oral administration of Ginsenoside Rg1 prevents cardiac toxicity induced by doxorubicin in mice through anti-apoptosis.* Oncotarget, 2017. **8**(48): p. 83792.

35. Nel, A., E. Ruoslahti, and H. Meng, *New Insights into "Permeability" as in the Enhanced Permeability and Retention Effect of Cancer Nanotherapeutics*. 2017, ACS Publications.

36. von Roemeling, C., et al., *Breaking down the barriers to precision cancer nanomedicine.* Trends in biotechnology, 2017. **35**(2): p. 159-171.

37. Kim, H.S. and D.Y. Lee, *Photothermal therapy with gold nanoparticles as an anticancer medication.* Journal of Pharmaceutical Investigation, 2017. **47**(1): p. 19-26.

38. Mocan, L., et al., *Selective ex vivo photothermal nano-therapy of solid liver tumors mediated by albumin conjugated gold nanoparticles.* Biomaterials, 2017. **119**: p. 33-42.

39. Sakr, T.M., et al., *In Silico-Based Repositioning of Phosphinothricin as a Novel Technetium-99m Imaging Probe with Potential Anti-Cancer Activity.* Molecules, 2018. **23**(2): p. 496.

40. Sakr, T.M., et al., *Preparation and biological profile of 99mTc-lidocaine as a cardioselective imaging agent using 99mTc eluted from 99Mo/99mTc generator based on Al–Mo gel.* Journal of Radioanalytical and Nuclear Chemistry, 2017. **314**(3): p. 2091-2098.

41. Saha, G.B., *Fundamentals of nuclear pharmacy*. 2010: Springer Science & Business Media.

42. Hou, X., M. Jensen, and S.P. Nielsen, *Use of 99mTc from a commercial 99Mo/99mTc generator as yield tracer for the determination of 99Tc at low levels.* Applied radiation and isotopes, 2007. **65**(5): p. 610-618.

43. Naqvi, S.A.R., et al., *Radiosynthesis and preclinical studies of 177Lu-labeled sulfadiazine: a possible theranostic agent for deep-seated bacterial infection.* Journal of Radioanalytical and Nuclear Chemistry, 2017. **314**(2): p. 1023-1029.

44. Notni, J. and H.J. Wester, *Re‐thinking the role of radiometal isotopes: Towards a future concept for theranostic radiopharmaceuticals.* Journal of Labelled Compounds and Radiopharmaceuticals, 2017.

45. Rashed, H., F. Marzook, and H. Farag, *99mTc-zolmitriptan: radiolabeling, molecular modeling, biodistribution and gamma scintigraphy as a hopeful radiopharmaceutical for lung nuclear imaging.* La radiologia medica, 2016. **121**(12): p. 935-943.

46. Zolle, I., *Technetium-99m pharmaceuticals*. 2007: Springer.

47. Sakr, T., M. Motaleb, and I. Ibrahim, *99mTc–meropenem as a potential SPECT imaging probe for tumor hypoxia.* Journal of Radioanalytical and Nuclear Chemistry, 2012. **292**(2): p. 705-710.

Preprints (www.preprints.org) | NOT PEER-REVIEWED | Posted: 18 August 2018 doi:10.20944/preprints201808.0331.v1

48. Isaacs, C.E., et al., *Epigallocatechin gallate inactivates clinical isolates of herpes simplex virus.* Antimicrobial agents and chemotherapy, 2008. **52**(3): p. 962-970.

49. Moses, M.A., et al., *The heat shock protein 90 inhibitor,(−)-epigallocatechin gallate, has anticancer activity in a novel human prostate cancer progression model.* Cancer Prevention Research, 2015. **8**(3): p. 249-257.

50. Gan, R.-Y., et al., *Absorption, metabolism, anti-cancer effect and molecular targets of epigallocatechin gallate (EGCG): An updated review.* Critical reviews in food science and nutrition, 2017: p. 1-18.

51. Mosmann, T., *Rapid colorimetric assay for cellular growth and survival: application to proliferation and cytotoxicity assays.* Journal of immunological methods, 1983. **65**(1-2): p. 55-63.

52. Gomha, S.M., S.M. Riyadh, and E.A. Mahmmoud, *Synthesis and anticancer activities of thiazoles, 1, 3-thiazines, and thiazolidine using chitosan-grafted-poly (vinylpyridine) as basic catalyst.* Heterocycles: an international journal for reviews and communications in heterocyclic chemistry, 2015. **91**(6): p. 1227-1243.

53. Essa, B., et al., *99m Tc-amitrole as a novel selective imaging probe for solid tumor: In silico and preclinical pharmacological study.* European Journal of Pharmaceutical Sciences, 2015. **76**: p. 102-109.

54. Rashed, H.M., R.N. Shamma, and E.B. Basalious, *Contribution of both olfactory and systemic pathways for brain targeting of nimodipine-loaded lipo-pluronics micelles: in vitro characterization and in vivo biodistribution study after intranasal and intravenous delivery.* Drug delivery, 2017. **24**(1): p. 181-187.

55. Abd-Elal, R.M., et al., *Trans-nasal zolmitriptan novasomes: in-vitro preparation, optimization and in-vivo evaluation of brain targeting efficiency.* Drug delivery, 2016. **23**(9): p. 3374-3386.

56. Nour, S.A., et al., *Intranasal brain-targeted clonazepam polymeric micelles for immediate control of status epilepticus: in vitro optimization, ex vivo determination of cytotoxicity, in vivo biodistribution and pharmacodynamics studies.* Drug delivery, 2016. **23**(9): p. 3681-3695.

57. Sakr, T., M. Motaleb, and W. Zaghary, *Synthesis, radioiodination and in vivo evaluation of ethyl 1, 4-dihydro-7-iodo-4-oxoquinoline-3-carboxylate as a potential pulmonary perfusion scintigraphic radiopharmaceutical.* Journal of Radioanalytical and Nuclear Chemistry, 2015. **303**(1): p. 399-406.

58. Katti, K.V., et al., *EGCG stabilized gold nanoparticles and method for making same*. 2016, Google Patents.

59. Mirza, A.Z. and H. Shamshad, *Preparation and characterization of doxorubicin functionalized gold nanoparticles.* European journal of medicinal chemistry, 2011. **46**(5): p. 1857-1860.

60. Elbialy, N.S., M.M. Fathy, and W.M. Khalil, *Preparation and characterization of magnetic gold nanoparticles to be used as doxorubicin nanocarriers.* Physica Medica: European Journal of Medical Physics, 2014. **30**(7): p. 843-848.

61. Curry, D., et al., *Adsorption of doxorubicin on citrate-capped gold nanoparticles: insights into engineering potent chemotherapeutic delivery systems.* Nanoscale, 2015. **7**(46): p. 19611-19619.

62. Hoshyar, N., et al., *The effect of nanoparticle size on in vivo pharmacokinetics and cellular interaction.* Nanomedicine, 2016. **11**(6): p. 673-692.

63. Chithrani, B.D., A.A. Ghazani, and W.C. Chan, *Determining the size and shape dependence of gold nanoparticle uptake into mammalian cells.* Nano letters, 2006. **6**(4): p. 662-668.

64. Kim, H.-S., Y.-S. Lee, and D.-K. Kim, *Doxorubicin exerts cytotoxic effects through cell cycle arrest and Fas-mediated cell death.* Pharmacology, 2009. **84**(5): p. 300-309.

65. Keizer, H., et al., *Doxorubicin (adriamycin): a critical review of free radical-dependent mechanisms of cytotoxicity.* Pharmacology & therapeutics, 1990. **47**(2): p. 219-231.

66. Kobayashi, H., R. Watanabe, and P.L. Choyke, *Improving conventional enhanced permeability and retention (EPR) effects; what is the appropriate target?* Theranostics, 2014. **4**(1): p. 81.

67. Kobayashi, H. and P.L. Choyke, *Super enhanced permeability and retention (SUPR) effects in tumors following near infrared photoimmunotherapy.* Nanoscale, 2016. **8**(25): p. 12504-12509.

68. Verhelle, A., et al., *Non-Invasive Imaging of Amyloid Deposits in a Mouse Model of AGel Using 99m Tc-Modified Nanobodies and SPECT/CT.* Molecular Imaging and Biology, 2016. **18**(6): p. 887-897.

69. Jaszczak, R.J., et al., *Improved SPECT quantification using compensation for scattered photons.* Journal of nuclear medicine: official publication, Society of Nuclear Medicine, 1984. **25**(8): p. 893-900.

70. Henze, M., et al., *Detection of tumour progression in the follow-up of irradiated low-grade astrocytomas: comparison of 3-[123 I] iodo-α-methyl-L-tyrosine and 99m Tc-MIBI SPET.* European journal of nuclear medicine and molecular imaging, 2002. **29**(11): p. 1455-1461.

71. Huang, X., et al., *Cancer cell imaging and photothermal therapy in the near-infrared region by using gold nanorods.* Journal of the American Chemical Society, 2006. **128**(6): p. 2115-2120.

72. Chen, J., et al., *Immuno gold nanocages with tailored optical properties for targeted photothermal destruction of cancer cells.* Nano letters, 2007. **7**(5): p. 1318-1322.

73. Ahn, H.-Y., et al., *Epigallocathechin-3 Gallate Selectively Inhibits the PDGF-BB–induced Intracellular Signaling Transduction Pathway in Vascular Smooth Muscle Cells and Inhibits Transformation ofsis-transfected NIH 3T3 Fibroblasts and Human Glioblastoma Cells (A172).* Molecular biology of the cell, 1999. **10**(4): p. 1093-1104.

74. Rodriguez, S.K., et al., *Green tea catechin, epigallocatechin‐3‐gallate, inhibits vascular endothelial growth factor angiogenic signaling by disrupting the formation of a receptor complex.* International Journal of Cancer, 2006. **118**(7): p. 1635-1644.

Preprints (www.preprints.org) | NOT PEER-REVIEWED | Posted: 18 August 2018 doi:10.20944/preprints201808.0331.v1

75. Sah, J.F., et al., *Epigallocatechin-3-gallate inhibits epidermal growth factor receptor signaling pathway evidence for direct inhibition of ERK1/2 and AKT kinases.* Journal of Biological Chemistry, 2004. **279**(13): p. 12755-12762.

76. Shimizu, M., et al., *EGCG inhibits activation of the insulin-like growth factor-1 receptor in human colon cancer cells.* Biochemical and biophysical research communications, 2005. **334**(3): p. 947-953.